A PLANAR PROBLEM IN THE BURNING OF AN AEROSOL OF A UNITARY FUEL IN A CLOSED REGION

P. B. Vainshtein, Yu. A. Morgunov,
and R. I. Nigmatulin

UDC 534.222.2

In the convective combustion of an aerosol, the speeds of the gas and combustion front are often much less than the speed of sound in the gas. In that case, the process can be examined within the framework of the homobaric approximation [1], in which one uses an equation for the homogeneity of the gas pressure in space instead of the momentum equation. One-dimensional treatments of convective aerosol combustion for bounded regions have been considered in [2-4] within the framework of the homobaric approximation. In [5], analogous problems were solved numerically, and it was shown that damped oscillations in the parameters occur at low fuel concentrations in a flow, with the oscillations occurring around the homobaric solution. In [6], results were presented briefly from the numerical solution of a one-dimensional problem on the combustion of coal dust suspended in air in a closed region.

Here we consider convective combustion in a square region for low fuel concentrations. The equation system is unclosed for two-dimensional motion in the homobaric approximation. It is closed by assuming that the motion is potential. The resulting solutions are compared with the numerical solution to the complete system of equations. The comparison shows that the assumption of potential behavior is correct. The characteristic streamline and isobar patterns are presented.

In [7], a numerical study was made of the planar nonstationary combustion of a cloud of unitary fuel particles in a half-space above a horizontal surface.

1. Formulation and Basic Equations. Consider planar two-dimensional flow of an aerosol. The equations of continuity for the gas and solid phases and for the conservation of the number of particles in unit volume take the form [1]

$$\frac{\partial \rho_1}{\partial t} + \nabla\cdot(\rho_1 \mathbf{V}_1) = J, \quad \frac{\partial \rho_2}{\partial t} + \nabla\cdot(\rho_2 \mathbf{V}_2) = -J, \quad \frac{\partial n}{\partial t} + \nabla\cdot(n\mathbf{V}_2) = 0, \tag{1.1}$$

where ρ_i, $V_i(u_i, v_i)$ $(i = 1, 2)$ are the mean densities and velocities of the corresponding phases, n is the number of particles in unit volume, and J is the mass combustion rate.

We examine low-density suspensions, where the volume content of the fuel can be neglected, and write the equations of motion as

$$\frac{\partial \rho_1 \mathbf{V}_1}{\partial t} + \frac{\partial}{\partial x}\rho_1 u_1 \mathbf{V}_1 + \frac{\partial}{\partial y}\rho_1 v_1 \mathbf{V}_1 + \nabla p = -\mathbf{f} + J\mathbf{V}_2, \tag{1.2}$$

$$\frac{\partial \rho_2 \mathbf{V}_2}{\partial t} + \frac{\partial}{\partial x}\rho_2 u_2 \mathbf{V}_2 + \frac{\partial}{\partial y}\rho_2 v_2 \mathbf{V}_2 = \mathbf{f} - J\mathbf{V}_2,$$

where p is gas pressure and $\mathbf{f}(f_x, f_y)$ is interfacial friction.

The following are the equations for the internal energy of the solid phase, the total energy of the mixture, and the equations of state correspondingly:

$$\frac{\partial \rho_2 e_2}{\partial t} + \nabla\cdot(\mathbf{V}_2\rho_2 e_2) = q - Je_{2s}, \tag{1.3}$$

$$\frac{\partial}{\partial t}(\rho_1 E_1 + \rho_2 E_2) + \nabla\cdot(\mathbf{V}_1(p + \rho_1 E_1)) + \nabla\cdot(\mathbf{V}_2\rho_2 E_2) = 0,$$

$$E_i = e_i + (u_i^2 + v_i^2)/2, \quad e_1 = c_V(T_1 - T_0),$$

$$e_2 = c_2(T_2 - T_0) + Q, \quad p = \rho_1^0 R_1 T_1, \quad \rho_2^0 = \text{const},$$

Moscow. Translated from Zhurnal Prikladnoi Mekhaniki i Tekhnicheskoi Fiziki, No. 6, pp. 103-110, November-December, 1985. Original article submitted July 9, 1984.

0021-8944/85/2606-0851$09.50

where e_1 and e_2 are the internal energies of the phases, whose temperatures are T_i, and Q is the reaction energy.

We assume that a particle ignites when its surface reaches a given decomposition (ignition) temperature T_S. To determine the mean-mass temperature of the particles T_S^* at which ignition occurs, we consider the heating of a spherical particle:

$$\rho_2 c_2 \frac{\partial T_2'}{\partial \tau} - \frac{1}{r^2}\frac{\partial}{\partial r}\left(\lambda_2 r^2 \frac{\partial T_2'}{\partial r}\right) = 0, \quad \left.\frac{\partial T_2'}{\partial r}\right|_{r=r_0} = \frac{\mathrm{Nu}\,(T_1 - T_{2\sigma}')}{2r_0}, \tag{1.4}$$

$$\left.\frac{\partial T_2'}{\partial r}\right|_{r=0} = 0, \quad T_2'(0, r) = T_{20}, \quad T_2 = 3/r_0^3 \int_0^{r_0} r^2 T_2' dr.$$

Here $T_{2\sigma}'$ is the current surface temperature and T_2 is the mean mass particle temperature. From (1.4) we get the value $T_2 = T_S^*$ at the time when the surface ignites ($T_{2\sigma}' = T_S$). In the range $\mathrm{Nu}(T_1 - T_S)/T_0$ from 0 to 400, the theoretical dependence of T_S^* on $\mathrm{Nu}(T_1 - T_S)/T_0$ is obtained from (1.4) by an inexplicit net method, which is approximated with an accuracy of 3% by

$$\frac{T_s^*}{T_0} = 1 + \left(\frac{T_s}{T_0} - 1\right)\exp\left(\frac{\lambda_1}{\lambda_2}\,\mathrm{Nu}\,\frac{T_s - T_1}{7T_0}\right). \tag{1.5}$$

The terms for the interaction between phases are

$$J = \begin{cases} 0, & T_2 < T_s^*, \\ \pi n d^2 \rho_2^0 u_s (p/p_0)^{\varphi}, & T_2 \geqslant T_s^*, \end{cases} \tag{1.6}$$

$$q = \begin{cases} \pi n d \lambda_1 \mathrm{Nu}_{12}(T_1 - T_2), & T_2 < T_s^*, \\ 0, & T_2 \geqslant T_s^*, \end{cases}$$

$$\mathrm{Nu}_{12} = 2 + 0{,}6\,\mathrm{Re}_{12}^{2/3}\mathrm{Pr}^{1/3}, \quad \mathrm{Re}_{12} = \frac{\rho_1^0 |\mathbf{V}_1 - \mathbf{V}_2| d}{\mu_1}, \quad \mathrm{Pr} = \frac{c_p \mu_1}{\lambda_1},$$

$$\mathbf{f} = \frac{n\pi d^2}{4} C_d \rho_1^0 \frac{|\mathbf{V}_1 - \mathbf{V}_2|(\mathbf{V}_1 - \mathbf{V}_2)}{2}, \quad C_d = \frac{24}{\mathrm{Re}_{12}} + \frac{4{,}4}{\mathrm{Re}_{12}^{0,5}} + 0{,}42,$$

where λ_1 and μ_1 are the thermal conductivity and viscosity of the gas; d, particle diameter; u_S, fuel combustion rate; Nu_{12}, Re_{12}, Pr, Nusselt, Reynolds, and Prandtl numbers for the relative flow around the particles; and C_d, coefficient of friction.

We consider the growth of convective combustion in a bounded region. Let the region G ($0 \leq x, y \leq \ell$) be filled with the aerosol, and in a certain part G_0 ($0 \leq x, y \leq x_0$), the temperature of the fuel particles is raised to $T_2 = T_S$ at the initial instant without raising the pressure, and combustion begins. The initial and boundary conditions are

$$t = 0 : \mathbf{V}_1 = \mathbf{V}_2 = 0, \; T_1 = T_0, \; \rho_1 = \rho_{10}, \; \rho_2 = \rho_{20},$$
$$n = n_0, \; T_2 = T_0((x, y) \in G \setminus G_0), \; T_2 = T_s((x, y) \in G_0), \tag{1.7}$$
$$t \geqslant 0 : \mathbf{V}_{1n}|_{\partial G} = 0,$$

where ∂G is the boundary of the region and $\mathbf{V}_{1n}$ is the velocity component normal to the boundary.

2. Convective Combustion in the Homobaric Approximation. After the start of combustion, the products penetrate into the unburned region under the pressure difference and heat the particles to the ignition temperature. If the mass content of the particles is small ($\rho_{20}/(\rho_{20} + \rho_{10}) \ll 1$), the effects of the particles on the gas motion are slight. Therefore, to describe the initial stage of motion, when the reaction time is less than the time for particle entrainment in the gas motion, we can consider the particles as immobile and neglect the effects of the friction between phases on the gas. The combustion propagation speed is defined by the dimensionless parameter [4]

$$\Pi = 6(\gamma - 1)\rho_{20} Q u_s l/\rho_{10} d a_0^3.$$

For small values of this parameter, the convective combustion rate is substantially less than the speed of sound, so the pressure has had time to equalize in the motion of the convective front in the bounded region and the process can be examined in the homobaric approximation. In the one-dimensional approximation, the velocity pattern is uniquely determined by the energy equation [2]. In the two-dimensional motion in the homobaric approximation, the equation system is unclosed, since the two equations for the gas momentum are replaced by one equation for the uniformity of the pressure p = p(t). To close the system, we assume that the flow is potential. This follows from the motion in that case being essentially acoustic, since it arises from small perturbations related to the distributed injection and heat production. In the next section, the assumption about potential flow in the essentially subsonic motion is confirmed by numerical solution of the complete equation system.

With these assumptions, the equations describing the mixture motion take the form

$$\begin{gathered} \mathbf{V}_2 = 0,\ \partial\rho_2/\partial t = -J,\ \partial n/\partial t = 0, \\ \partial\rho_2 e_2/\partial t = q - J e_{2s},\ \partial\rho_1/\partial t + \nabla\cdot(\mathbf{V}_1\rho_1) = J, \\ \mathbf{V}_1 = \nabla\varphi,\quad \nabla^2\varphi = \Psi,\quad \Psi = \frac{\gamma-1}{\gamma p}\left(\frac{1}{1-\gamma}\frac{dp}{dt} + JQ\right). \end{gathered} \tag{2.1}$$

The following condition for the potential follows from the boundary conditions of (1.7):

$$\partial\varphi/\partial n|_{\partial G} = 0. \tag{2.2}$$

We consider two limiting cases: combustion occurs only in the initiation zone G_0, and the propagation of the hot gases does not ignite the particles outside G_0; or alternatively, the particles ignite instantaneously at the convective front outside the ignition zone. We integrate the last equation i (2.1) throughout the region and use the boundary conditions of (2.2) together with the integral Green's formula to get the pressure-increase law for the first form:

$$\frac{dp}{dt} = JQ(\gamma - 1)\frac{x_0^2}{l^2}.$$

In the second form, the equations for the area S_w of the combustion zone are

$$\frac{dS_w}{dt} = \int_G \nabla^2\varphi\, d\tau.$$

In the initial stage, the burnup of the solid may be neglected [4], i.e., we put J = const in formula (1.6) for the mass burning rate. Then we get the pressure increase from

$$\frac{dp}{dt} = JQ(\gamma - 1)\frac{S_w}{l^2},\quad \frac{dS_w}{dt} = \frac{\gamma-1}{\gamma p}\left(\frac{1}{\gamma-1} + JQ\right),$$

$$t = 0:\ p = p_0,\quad S_w = x_0^2.$$

The solution to the Neumann problem of (2.1) and (2.2) for the square region is sought as Fourier series. The complete system of eigenfunctions for that case is [8]

$$\theta_{ij}(x, y) = \cos\left(\frac{i\pi x}{l}\right)\cos\left(\frac{j\pi y}{l}\right)\quad (i, j = 1, 2)\ .$$

The coefficients in the expansion for the potential

$$\varphi = \sum_{0,0}^{\infty} c_{ij}\theta_{ij}(x, y)$$

are determined from

$$c_{ij} = \frac{1}{\lambda_{ij}}\int_0^l\int_0^l \Psi\theta_{ij}(x, y)\, dxdy. \tag{2.3}$$

We apply Green's formula to (2.3) to get

$$c_{ij} = \frac{l}{\lambda_{ij} i\pi} \oint_{\partial G_0} \Psi \sin\left(\frac{i\pi x}{l}\right) \cos\left(\frac{j\pi y}{l}\right) dy. \tag{2.4}$$

In the calculations, we use a finite segment of the Fourier series ($0 \leq i, j \leq N$); the number N is chosen such that the relative error is not more than 1%. In the form given below, N = 15.

The calculations were performed for a model fuel with the following thermodynamic data and conditions [5]:

$\rho_{10}^0 = 1{,}29$ kg/m^3, $\rho_{20}^0 = 1550$ kg/m^3,
$R_1 = 287$ m^2/sec^2·g, $c_{p1} = 1000$ m^2/sec^2·g, $c_{V1} = 713$ m^2/sec^2·g,
$c_2 = 1466$ m^2/sec^2·g, $T_s = 473$ K, $T_0 = 273$ K,
$\mu_1 = 1{,}7 \cdot 10^{-5}$ kg/m·sec, $\lambda_1 = 2{,}57 \cdot 10^{-2}$ kg·m/sec^3·g, $\lambda_2 = 0{,}687$ kg·m/sec^3·g

We consider the combustion for d = 0.5 mm and $\rho_{20} = 0.13$ kg/m^3 in a region $\ell = 0.84$ m, $x_0 = 0.25\ell$; Fig. 1 shows the gas flow lines together with the numbered level lines for the modulus of the velocity at the initial instant (the dashed lines are $X = x/\ell$, $Y = y/\ell$). The modulus of the velocity is derived from $|V_1| = i\ 0.159$ m/sec, where i is the line number. The gas emerging from the combustion zone flows outwards somewhat. The cold gas compressed by the combustion products moves towards the corner opposite to the combustion zone. It is evident from (2.4) that the streamline pattern is entirely determined by the shape of the combustion zone, and it is independent of time for the first form. The maximum gas speed occurs at the boundary of the combustion zone. The velocity $\mathbf{V}_1(x, y, t)$ at any instant is defined by

$$\mathbf{V}_1(x, y, t) = \mathbf{V}_1(x, y, 0) A_1(t)/A_1(0),$$

where $A_1(t)$ is shown in Fig. 2 (line 7). In the case of instantaneous ignition, the combustion zone enlarges at the convective front. The flow pattern as the combustion zone enlarges varies only slightly. The current lines deviate somewhat from their initial positions, but they still emerge from the origin and terminate at the opposite corner. The maximum velocity occurs at the boundary of the combustion zone. The dashed lines in Fig. 1 show the positions of the flame front at the instants t = 0, 85, and 170 msec (lines 1-3). Figure 2 shows the dependence of the pressure $\Delta P = 10^3\ (p - p_0)/p_0$ on time ($\tau = t/t_0$, $t_0 = d/2u_s$) for the case with the fixed combustion zone (line 1) and the case with instantaneous ignition (line 2), as well as the time dependence of $|V_1| = |V_1|/V_0$ at a given point (X = 0.25, Y = 0.2, $V_0 = 0.14$ m/sec (line 4), and the time dependence of the density of the solid phase in the combustion zone ($R_2 = 20(\rho_2/\rho_{20})$) (line 6).

The complete system (1.1)-(1.7) was solved numerically in three stages with allowance for the wave effects: 1) the solution was obtained neglecting the phase-interaction terms (J, q, f), with the Lax–Wendroff two-step method used in the difference approximation; 2) the solution was refined with allowance for the phase-interaction terms by means of an explicit scheme of the first order of accuracy; and 3) smoothing was applied in the regions where there is an irregularity in the solution of [9].

We consider combustion with the above parameters. In Figs. 3 and 4 a-h correspondingly, we show the streamlines and isobars for t = 1.8; 2.9; 4.3; 4.6; 5.8; 6.7; 8.5; 46 msec, with the numbers on the isobars the pressure increments relative to the initial value in percent. Figure 2 shows the time dependence of the pressure (line 3) at the point (0) and the horizontal velocity component at the point (0.25, 0.2) (line 5). It is evident that the parameters oscillate. One can establish the mode of oscillation by considering the streamlines and isobars at different instants, which show the successive states.

Before the perturbation has reached the walls of the region, the streamlines are almost straight, with the minor curvature due to the initiation zone not having circular symmetry. The isobars are almost circles (a). At t = 2 msec, the pressure perturbation attains the

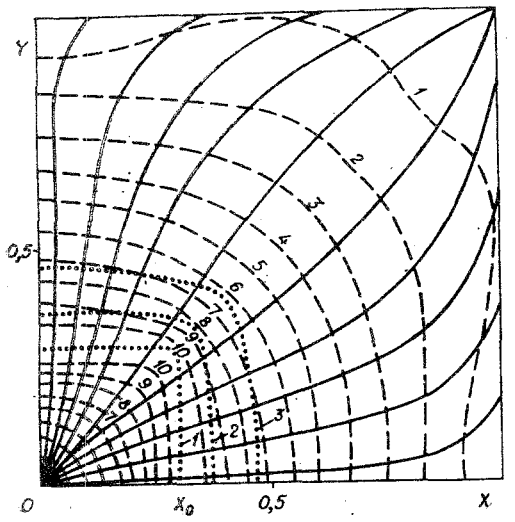

Fig. 1

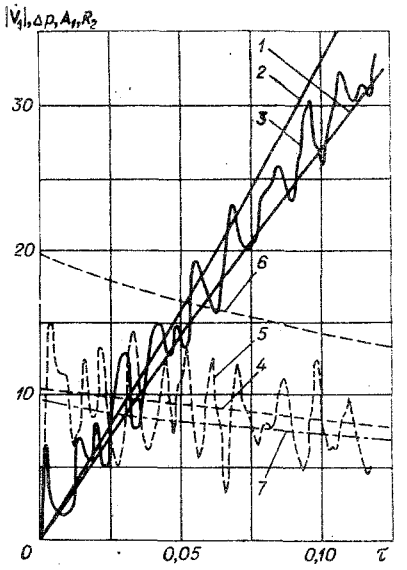

Fig. 2

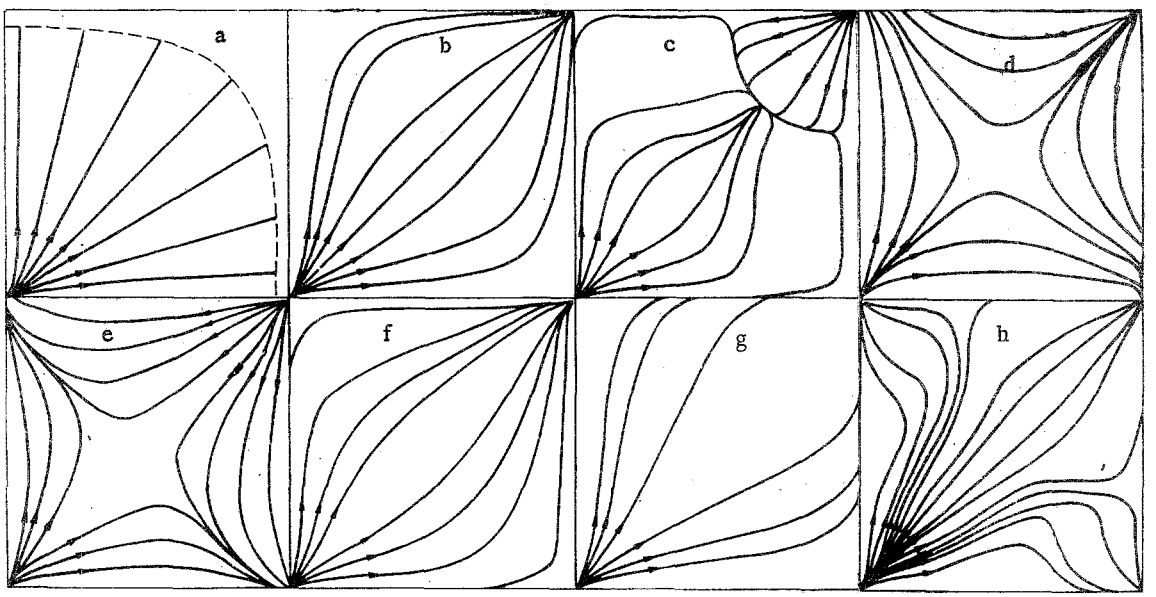

Fig. 3

opposite walls (b). Reflected waves begin to advance from the nearest corners. At the same time, the streamlines become curved and rotate towards the remote corner. At t = 2.8 msec, the perturbation reaches the far corner, where the pressure increases, the gas is retarded, and a zone of reverse flow arises. The zones of reverse and main flow are evident from the patterns. At that time, the compression waves are still advancing from the two opposing nearer corners, and the streamlines converge towards the diagonal joining the remote corner to the initiation zone. When these waves meet, an increase in pressure occurs along that diagonal, which rotates the flows towards the wall (d). The compression wave reflected from the far corner continues to move towards the initiation zone, and the region of return flow enlarges (e). When the wave moving from the far corner attains the initiation zone and the waves it has produced after reflection from the near corners meet at the center, the gas flow in the entire region takes the direction from the initiation zone to the opposite corner, and the flow pattern is close to the initial one, but the pressure throughout the region is higher (f). The difference is related to the above wave interaction. Further, the compression wave moves towards the far corner (g). Therefore, there is oscillatory gas motion. Subsequently, the motion, reflection, and interaction of the large number of compression waves causes the picture to be no longer regular. Therefore, a difference from the one-dimensional case [4] is that the motion is not periodic. One of the flow patterns is

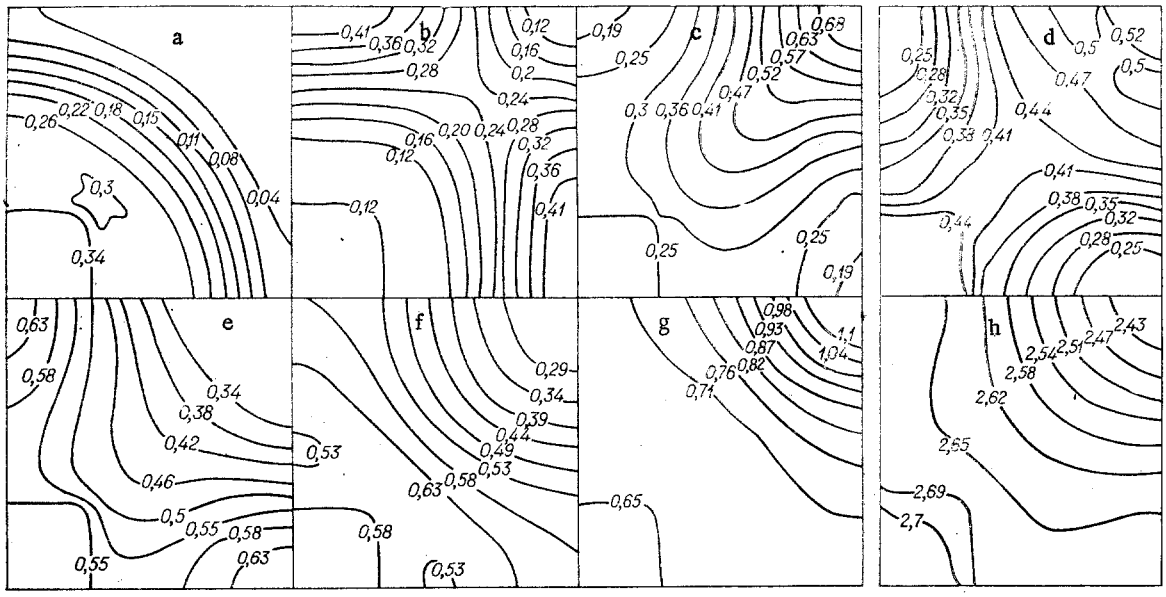

Fig. 4

shown in parts h of Figs. 3 and 4. Frictional forces, the retarding force in gas injection, and the reduction of the injection due to fuel burnup cause these oscillations to be damped. The flow pattern becomes similar to that in the homobaric approximation. In that form, the combustion occurs only in the initiation zone, and the flame front is hardly displaced. However, there are slight oscillations in the front itself because of the oscillations in gas speed at it.

The pressure and velocity fluctuations occur around the homobaric solution derived on the assumption of potential flow in the first form (compares lines 1 and 3 or 4 and 5 in Fig. 2). The solution with instantaneous ignition at the convective front gives pressures higher than those obtained from solving the complete system.

Calculations from the complete system (1.1)-(1.7) enable one to derive the values for the velocity rotor at each point: $\omega = (\partial y/\partial y - \partial v/\partial x)/2$. In the above form, $\max|\omega| \sim 10^{-2}$ sec^{-1}. Then the corresponding nonpotential velocity component is [10] given by

$$\mathbf{V}_\omega(x, y) = \int_G\int \frac{\boldsymbol{\omega}\times\mathbf{r}}{|\mathbf{r}|^2}d\tau,$$

according to which we have the bound

$$|\mathbf{V}_\omega| = \left|\int_G\int \frac{\boldsymbol{\omega}\times\mathbf{r}}{|\mathbf{r}|^2}\,d\tau\right| \leqslant \max_G|\omega|\,l.$$

Then $|\mathbf{V}_\omega| \leq 10^{-2}$ m/sec. Therefore, in this case (low concentrations and high heat contents of the fuel), the velocity generated by the vortex represents a slight correction to the potential velocity component ($|\mathbf{V}_1| \sim 1.5$ m/sec).

LITERATURE CITED

1. R. I. Nigmatulin, Principles of the Mechanics of Heterogeneous Media [in Russian], Nauka, Moscow (1978).
2. P. B. Vainshtein and R. I. Nigmatulin, "Homobaric aerosol flows (with homogeneous pressure) in the presence of heterogeneous physicochemical transformations," Dokl. Akad. Nauk SSSR, 249, No. 1 (1981).
3. P. B. Vainshtein, "Convective combustion of unitary-field aerosols," Izv. Akad. Nauk SSSR, Mekh. Zhidk. Gaza, No. 5 (1980).
4. P. B. Vainshtein, "Theory of convective combustion of unitary-fuel aerosols," Izv. Akad. Nauk SSSR, Mekh. Zhidk. Gaza, No. 6 (1980).
5. P. B. Vainshtein and Yu. A. Morgunov, "A numerical study of the combustion of unitary-fuel aerosols in bounded regions," in: Nonstationary Flow of Multiphase Systems Involving Physicochemical Transformations [in Russian], Moscow State Univ. (1983).

6. V. A. Levin, J. V. Tunik and P. Wolanski, "Model matematyczny procesu wybuchy mieszaniy pylowo-powietrznej," Biuletyn Informacji Technicznej, 23, No. 3-4 (1980).
7. G. M. Makhviladze and O. I. Melikhov, "The combustion of an aerosol cloud above a planar horizontal surface," Khim. Fiz., No. 8 (1983).
8. R. Courant and D. Hilbert, Methods of Mathematical Physics [Russian translation], Vols. 1, 2, GITTL, Moscow–Leningrad (1981).
9. I. Sh. Akhatov and P. B. Vainshtein, "Nonstationary modes of combustion for porous powders," Fiz. Goreniya Vzryva, No. 3 (1983).
10. L. I. Sedov, The Mechanics of Continuous Media [in Russian], Vol. 2, Nauka, Moscow (1976).

ACCELERATION WAVE IN A GAS–SOLID PARTICLE MIXTURE WITH CONSIDERATION OF FUSION

A. V. Fedorov

UDC 532.529

A flow of gas mixed with solid particles occurs in many technological processes, in particular, in detonation deposition of finely dispersed metal particles on the surfaces of machine parts. The working substance (gas at high pressure and temperature) has sufficiently high state parameters so that fusion of the particles being driven occurs. This fusion may be of a nonequilibrium character, so that it is of interest to consider problems which develop in high velocity motion of such mixtures with consideration of this process.

The equations describing propagation of plane waves in an air-dispersed mixture of gas and solid particles at temperatures of the continuous phase sufficient for phase transition have the form [1, 2]

$$\partial x/\partial X = \rho_0 v,\ \partial\xi/\partial t = \varkappa = -(1/\tau)(\xi - \xi e),$$
$$\partial p/\partial X + \rho_0 \partial u/\partial t = 0,\ \partial e/\partial t + p\partial v/\partial t = 0,$$
$$e = e(S, v, \xi),\ p = -e_v(S, v, \xi),\ T = e_S(S, v, \xi),$$

where the Cartesian component x describing the motion of the medium is a function of the position of a point at the initial moment X and the current time t, i.e., $x = x(X, t)$; ρ_0 is the initial density of the mixture; v, p, u, e, T, S are the specific volume, pressure, velocity, internal energy, temperature, and entropy of the mixture; ξ is the relative mass concentration of the liquid phase; $\xi_e = \xi_e(S, v)$ is the equation of equilibrium fusion; τ is the relaxation time of the fusion process.

We will assume that at the initial moment the mixture has the following parameter values

$$v = v_0,\ \xi = \xi_0,\ S = S_0,\ x = X.$$

Following [3], we will define a second-order wave as a singularity in the flow propagating along the line $y = y(Y, T)$ on which $x(X, t)$ may have discontinuities in its second derivatives, while $x(X, t)$, $S(X, t)$, $\xi(X, t)$ have continuous first derivatives. Second-order waves are called acceleration waves.

Thus, by definition, in an acceleration wave the equations

$$[x] = [v] = [u] = [S] = [\xi] = 0,\ [\varphi] = \varphi_1 - \varphi_2$$

are satisfied.

Using the equation of state and the kinetic and energy equations, we find

Novosibirsk. Translated from Zhurnal Prikladnoi Mekhaniki i Tekhnicheskoi Fiziki, No. 6, pp. 111-113, November-December, 1985. Original article submitted September 26, 1984.

0021-8944/85/2606-0857$09.50